Galvanomagnetic Effects in *n*-Type Silicon*†

W. E. KRAG
Lincoln Laboratory, Massachusetts Institute of Technology, Lexington, Massachusetts
(Received November 3, 1959)

The galvanomagnetic effects in *n*-type silicon have been investigated experimentally and theoretically at 77°K and 300°K. The samples ranged in resistivity from 0.2 to 27 ohm-cm (at room temperature). Measurements of the field dependence from 0.5 to 22 kilogauss of the Hall coefficient and the magnetoresistance for several orientations are presented, as well as measurements of the angular dependence of the magnetoresistance and planar Hall effects at similar fields. A number of theoretical calculations using a constant relaxation time in the manner of Gold and Roth (1957) are presented which show the effect on the coefficients of a change in the mass anisotropy K_m. The Boltzmann transport equation, and collision times of the form

$$\nu_l = I_l \mathcal{E}^{-\frac{1}{2}} + L\mathcal{E}^{\frac{1}{2}} + N,$$
$$\nu_t = I_t \mathcal{E}^{-\frac{1}{2}} + L\mathcal{E}^{\frac{1}{2}} + N,$$

where ν_l and ν_t are the longitudinal and transverse collision times, I_l, I_t, L, and N are constants and $\mathcal{E}$ is the energy, have been used to calculate the galvanomagnetic coefficients for different amounts of lattice, ionized impurity and neutral impurity scattering, and for different anisotropies of the ionized impurity scattering. The various components of the collision frequency were taken from available theoretical work. Detailed comparisons of the experimental data and the theoretical calculations are presented which show that the assumption of a constant collision frequency allows one to predict qualitatively all the field dependencies and symmetries which are found experimentally. It is also shown that with an anisotropic, energy dependent collision frequency the quantitative agreement with experiment is considerably improved, especially with regard to the behavior of samples of different resistivities.

I. INTRODUCTION

MEASUREMENTS of the magnetoresistance have been used extensively to ascertain the structure of the band edges in various semiconductors,[1] and, more particularly for germanium and silicon, the effective masses and the mass anisotropy. For germanium and silicon it has been amply shown that the band edges have the form of ellipsoids along the [111] and [100] axes, respectively.[2,3] For these two elements the mass anisotropy has been measured rather directly at 4.2°K. Experimental results seem to indicate that for both germanium and silicon the mobility anisotropy is about the same at 300°K as at 4.2°K but lower at intermediate temperatures.[1,4,5] This has been attributed to an anisotropy of the ionized impurity scattering.[4]

The Hall coefficient has been used primarily to obtain carrier and impurity concentrations for use in energy gap calculations and for mobility measurements.[6] When measured as a function of temperature this gives considerable information about the scattering processes.[6–9]

There has been much theoretical work done on various scattering processes.[6] In particular lattice scattering has been thoroughly investigated[10,11] and equations have been derived for ionized[12,13] and neutral impurity scattering.[14,15] This theoretical work has been directed principally at gaining an understanding of the temperature and resistivity dependence of the measured carrier mobility. Primary attention in these calculations has been paid to germanium and silicon.

It seemed desirable to have further detailed measurements of the galvanomagnetic coefficients in silicon available for comparison with theoretical work. The following report is an attempt to fit a set of detailed galvanomagnetic measurements by using available theoretical work.

II. THEORY

The formal theory of conductivity for an ellipsoidal energy surface and an energy dependent anisotropic collision time can be developed in the manner of Shibuya[16] and Bullis[17] to obtain the conductivity tensor for the current carriers on a single ellipsoidal energy surface. The requirements are that the relaxation time be expressed as a tensor which is diagonal in the same coordinates as the mass tensor, that the electric field be weak, that the electron concentration be low enough so that the Boltzmann distribution may be used, and that there be no spatial effects such as temperature gradients or concentration gradients in the material.[16,17]

* The work reported in this paper was performed at Lincoln Laboratory, a center for research operated by Massachusetts Institute of Technology with the joint support of the U. S. Army, Navy, and Air Force.

† This paper is abstracted from a thesis presented to the Department of Physics, Massachusetts Institute of Technology, in partial fulfilment of the requirements for the Degree of Doctor of Philosophy.

[1] M. Glicksman, *Progress in Semiconductors* (Heywood and Company, London, 1958), Vol. 3, p. 1.
[2] B. Lax, Revs. Modern Phys. **30**, 122 (1958).
[3] G. Dresselhaus, A. F. Kip, and C. Kittel, Phys. Rev. **98**, 368 (1955).
[4] C. Goldberg, Bull. Am. Phys. Soc. **2**, 65 (1957).
[5] W. M. Bullis, Phys. Rev. **109**, 292 (1957).
[6] F. J. Blatt, *Solid-State Physics*, edited by F. Seitz and D. Turnbull (Academic Press, New York, 1957), Vol. 4, p. 200.
[7] E. Conwell, Proc. Inst. Radio Engrs. **46**, 1218 (1958).
[8] H. Brooks, *Advance in Electronics and Electron Physics*, edited by L. Marton (Academic Press, Inc., New York, 1955), Vol. 7, p. 87.
[9] C. Herring, Bell System Tech. J. **34**, 237 (1955).
[10] C. Herring, T. H. Geballe, and J. E. Kunzler, Phys. Rev. **111**, 36 (1958).
[11] C. Herring and E. Vogt, Phys. Rev. **101**, 944 (1956).
[12] E. Conwell and V. Weisskopf, Phys. Rev. **77**, 388 (1950).
[13] N. Sclar, Phys. Rev. **104**, 1548 (1956).
[14] C. Erginsoy, Phys. Rev. **79**, 1013 (1950).
[15] N. Sclar, Phys. Rev. **104**, 1559 (1956).
[16] M. Shibuya, Phys. Rev. **95**, 1385 (1954).
[17] W. M. Bullis, thesis, Massachusetts Institute of Technology, 1956 (unpublished).

There is no restriction on the value of the magnetic field.[16] With the distribution function expanded to first order:

$$f=f_0-\phi(\partial f_0/\partial \mathcal{E}), \tag{2.1}$$

where f_0 is the equilibrium distribution, $\phi=\mathbf{G}\cdot\nabla_p\mathcal{E}$, and $\nabla_p\mathcal{E}$ is the group velocity of the electrons, the Boltzmann transport equation may be solved for the distribution function with the result[17,18]

$$\mathbf{G}=\frac{-e\boldsymbol{\tau}\cdot[\mathbf{E}-e(\boldsymbol{\tau}\cdot\mathbf{E}\cdot\mathbf{w})\times\mathbf{B}+e^2(\mathbf{E}\cdot\mathbf{B})(\boldsymbol{\eta}\cdot\mathbf{B})]}{1+e^2(\boldsymbol{\eta}\cdot\mathbf{B})\cdot\mathbf{B}}. \tag{2.2}$$

In Eq. (2.2), e is the electronic charge, $\boldsymbol{\tau}$ is the relaxation time tensor, $\mathbf{E}$ is the electric field, $\mathbf{w}$ is the reciprocal of the mass tensor $\mathbf{m}$, $\mathbf{B}$ is the magnetic field, and $\boldsymbol{\eta}=\mathbf{m}\cdot\boldsymbol{\nu}/|m||\nu|$ where $\boldsymbol{\nu}=\boldsymbol{\tau}^{-1}$ and $|m|$ and $|\nu|$ are the determinants of their respective tensors.

With this distribution function the current density and therefore the conductivity tensor can be calculated for a single ellipsoidal energy surface.

In the case of silicon there are six ellipsoids of revolution oriented such that the axes of rotation are along the [100] axes.[19] When the conductivity components are summed over all of the ellipsoids the conductivity tensor is[18]:

$$\sigma_{ij}=-\frac{4}{3\pi^{\frac{1}{2}}}\frac{en}{(kT)^{\frac{3}{2}}}\int_0^\infty [\ ]_{ij}\mathcal{E}^{\frac{3}{2}}\exp(-\mathcal{E}/kT)d\mathcal{E}, \tag{2.3}$$

where

$$[\ ]_{11}=\frac{a_l+B_1^2a_t^2a_l}{1+a_ta_l[B_2^2+B_3^2+(a_t/a_l)B_1^2]}+\frac{a_t+B_1^2a_t^2a_l}{1+a_ta_l[B_3^2+B_1^2+(a_t/a_l)B_2^2]}+\frac{a_t+B_1^2a_t^2a_l}{1+a_ta_l[B_1^2+B_2^2+(a_t/a_l)B_3^2]},$$

$$[\ ]_{12}=\frac{-B_3a_ta_l+B_2B_1a_t^2a_l}{1+a_ta_l[B_2^2+B_3^2+(a_t/a_l)B_1^2]}+\frac{-B_3a_ta_l+B_2B_1a_t^2a_l}{1+a_ta_l[B_3^2+B_1^2+(a_t/a_l)B_2^2]}+\frac{-B_3a_t^2+B_1B_2a_t^2a_l}{1+a_ta_l[B_1^2+B_2^2+(a_t/a_l)B_3^2]},$$

and by permuting the subscripts 1, 2, 3 and using the Onsager relation,[20] $\sigma_{ij}(\mathbf{B})=\sigma_{ji}(-\mathbf{B})$, the other components of the conductivity tensor are easily obtained. In these expressions n is the electron concentration, k is the Boltzmann constant, T the absolute temperature, B_i is the component of the magnetic field along the ith axis and $a_{t(l)}=[e\tau_{t(l)}/m_{t(l)}]$, $\tau_{t(l)}=1/\nu_{t(l)}$ is the relaxation time transverse (parallel) to the major axis of the ellipsoidal energy surface. τ_t and τ_l are not necessarily the same, either in energy dependence or magnitude.

To obtain the galvanomagnetic coefficients the conductivity tensor is evaluated numerically and then inverted to give the resistivity tensor. The components of the resistivity tensor are then used to evaluate the galvanomagnetic coefficients from the following expressions.[17] For the magnetoresistance:

$$\Delta\rho/\rho_0=(\rho-\rho_0)/\rho_0=[(\mathbf{E}\cdot\mathbf{J})_B/(\mathbf{E}\cdot\mathbf{J})_{B=0}]-1,$$

the Hall coefficient

$$R=(\mathbf{E}\cdot\mathbf{J}\times\mathbf{B})/(\mathbf{J}\times\mathbf{B})^2, \tag{2.4}$$

and the Planar Hall coefficient

$$P=\frac{\mathbf{E}\cdot[(\mathbf{J}\times\mathbf{B})\times\mathbf{J}]}{(\mathbf{J}\times\mathbf{B})^2(\mathbf{J}\cdot\mathbf{B})}.$$

In these expressions the right-hand sides reduce to expressions involving only the components of the resistivity tensor ρ_{ij} (which are functions of the magnetic field) and direction cosines of the magnetic field.

A simple approximation which can be quite useful is that of a constant mean free time, independent of the electron energy.[21] Considerable use has been made of this approximation in evaluating cyclotron resonance

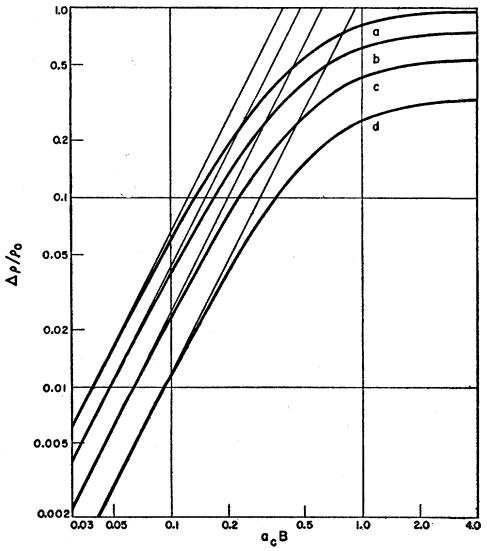

FIG. 1. Field dependence of the magnetoresistance $\Delta\rho/\rho_0$ for $J_{[110]}B^{[001]}=J_{[100]}B^{[001]}$. Theoretical—$\tau$=constant, (a) $K=6.2$, (b) $K=5.2$, (c) $K=4.2$, (d) $K=3.2$ (straight lines are extensions of the low field square law behavior).

[18] W. E. Krag, thesis, Massachusetts Institute of Technology, 1959 (unpublished).

[19] R. N. Dexter, B. Lax, A. F. Kip, and G. Dresselhaus, Phys. Rev. **96**, 222 (1954).

[20] L. Onsager, Phys. Rev. **38**, 2265 (1931).

[21] L. Gold, Phys. Rev. **99**, 596 (1955).

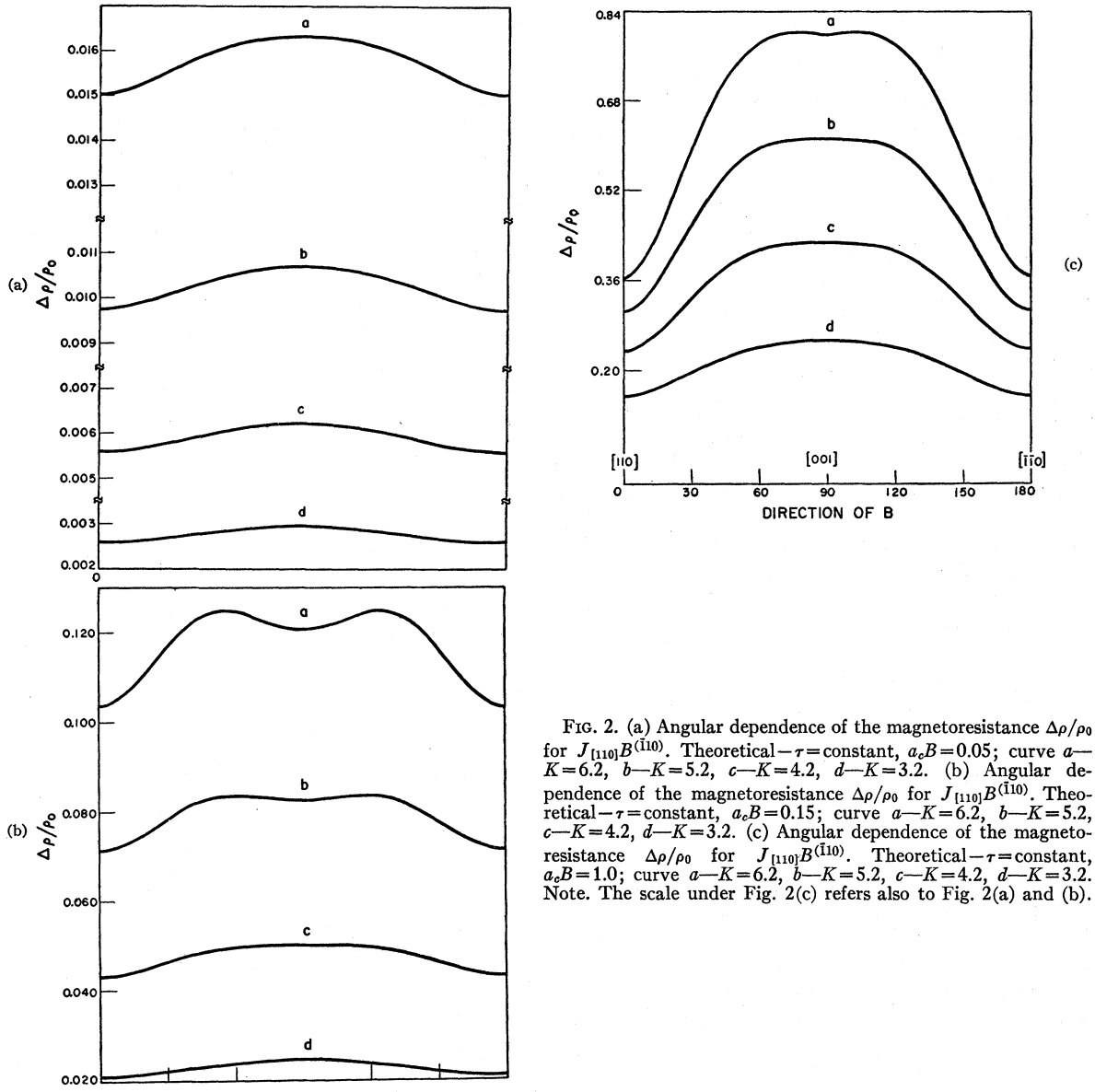

FIG. 2. (a) Angular dependence of the magnetoresistance $\Delta\rho/\rho_0$ for $J_{[110]}B^{(\bar{1}10)}$. Theoretical—τ=constant, $a_eB=0.05$; curve a—$K=6.2$, b—$K=5.2$, c—$K=4.2$, d—$K=3.2$. (b) Angular dependence of the magnetoresistance $\Delta\rho/\rho_0$ for $J_{[110]}B^{(\bar{1}10)}$. Theoretical—τ=constant, $a_eB=0.15$; curve a—$K=6.2$, b—$K=5.2$, c—$K=4.2$, d—$K=3.2$. (c) Angular dependence of the magnetoresistance $\Delta\rho/\rho_0$ for $J_{[110]}B^{(\bar{1}10)}$. Theoretical—τ=constant, $a_eB=1.0$; curve a—$K=6.2$, b—$K=5.2$, c—$K=4.2$, d—$K=3.2$. Note. The scale under Fig. 2(c) refers also to Fig. 2(a) and (b).

experiments[22] and also in galvanomagnetic experiments.[5,17,18,21,22–26] With this approximation the calculations are, of course, much simplified. The bracketed terms in Eq. (2.3) are independent of the energy and can therefore be taken outside the integral and evaluated directly. The integral itself is a gamma function of order $\frac{5}{2}$.

For energy dependent collision frequencies the integrals have to be evaluated numerically for each case. All of the computational work was done with an IBM-704 computer. Six figure accuracy was maintained throughout.

In the theoretical calculations attention was largely restricted to the case of a current in a [100] or [110] direction and a magnetic field in an [001] direction. The advantages of this case are (1) it is a high symmetry direction and the $\mathfrak{d}$ tensor reduces to 5 nonzero components, (2) the magnetoresistance is high in this orientation, and is therefore sensitive to changes in the mass anisotropy K_m and/or the scattering functions, and (3) the curve of the Hall coefficient versus magnetic field has a minimum, which is useful for comparisons of experiment and theory.

Consider first the calculations of the galvanomagnetic coefficients for the case of a constant mean free time.

[22] H. J. Zeiger, B. Lax, and R. N. Dexter, Phys. Rev. **105**, 495 (1956).
[23] L. Gold and L. M. Roth, Phys. Rev. **99**, 1655 (1955).
[24] L. Gold and L. M. Roth, Phys. Rev. **103**, 61 (1956).
[25] L. Gold and L. M. Roth, Phys. Rev. **107**, 358 (1957).
[26] W. M. Bullis and W. E. Krag, Phys. Rev. **101**, 580 (1956).

These have been calculated extensively for $K=5.2$,[23–25] but it is interesting to calculate the coefficients for other values of the mass anisotropy. Figure 1 shows that, as expected, the magnetoresistance increases as the mass anisotropy increases. Figure 1 is typical of the effect of increasing anisotropy on the magnetoresistance {except that the longitudinal magnetoresistance along a cubic ([100]) axis was zero in every case both for constant τ and energy dependent τ}. The variable $a_cB=eB\tau_c/m_l$ is the abscissa scale for all of the constant τ curves. Figure 2 shows the angular dependence of the magnetoresistance for one of the more interesting orientations. Note that the minimum at the [001] direction is present only at intermediate fields, and not at high or low magnetic fields, and that it also disappears for low mass anisotropies. Magnetoresistance calculations for other configurations of the current and magnetic field showed much the same behavior as found by Gold and Roth.[25] The anisotropy of the magnetoresistance as well as the magnitude decreases for low values of magnetic field (a_cB) as well as for low values of the mass anisotropy.

In considering the Hall coefficients several points should be remembered. First, it is well known that the high field limit of the Hall coefficient is equal to $R_\infty=1/ne$ for a one carrier system, where n is the number of carriers.[16] However, since the low field limit, but not the high field limit of the Hall coefficient, is experimentally accessible in n-type silicon, all but one of the curves are normalized to the low field values. Second, for spherical energy surfaces and a constant collision frequency the Hall coefficient is independent of the magnetic field and equal to its high field value (the magnetoresistance is zero for this case). And third, for cubic systems the high and low field limits of the Hall coefficients are independent of the configuration of the various orientation parameters,[9] but the low field limit depends on the mass anisotropy and, as will be shown later, on the scattering functions. Figure 3 shows the behavior of the Hall coefficient normalized to the low field limit as a function of field for several mass anisotropy ratios (and constant τ) for two transverse configurations of the current and magnetic field. The appearance of a minimum in the field dependence of the Hall coefficient depends strongly on the relative orientations of the current, magnetic field and the crystal axes, and that the depth of the minimum is a function of the mass anisotropy.

As seen in Fig. 4 the planar Hall coefficient P/ρ_0 also depends on the mass anisotropy and on the various orientation parameters.

The calculations making use of a constant collision frequency do not, of course, correspond to the physical situation. They do, however, as we shall see, show all the features which are found experimentally, and being easily and quickly calculable on even a simple computer such as the Royal McBee LGP-30, would seem to be of considerable use, especially in exploratory calculations. For more realistic calculations an energy dependent collision frequency is required.

Of the many types of possible scattering mechanisms there are three that are usually important in good crystals at normal temperatures; lattice scattering, ionized impurity scattering, and neutral impurity scattering. At room temperatures lattice scattering is usually the dominant mechanism and neutral impurity scattering can probably be neglected. In silicon at liquid nitrogen temperatures, however, both lattice and ionized impurity scattering can be important, and in many cases, neutral impurity scattering plays a significant role. Usually the scattering mechanisms are assumed to act independently and a mobility is calculated for each process separately. However, this

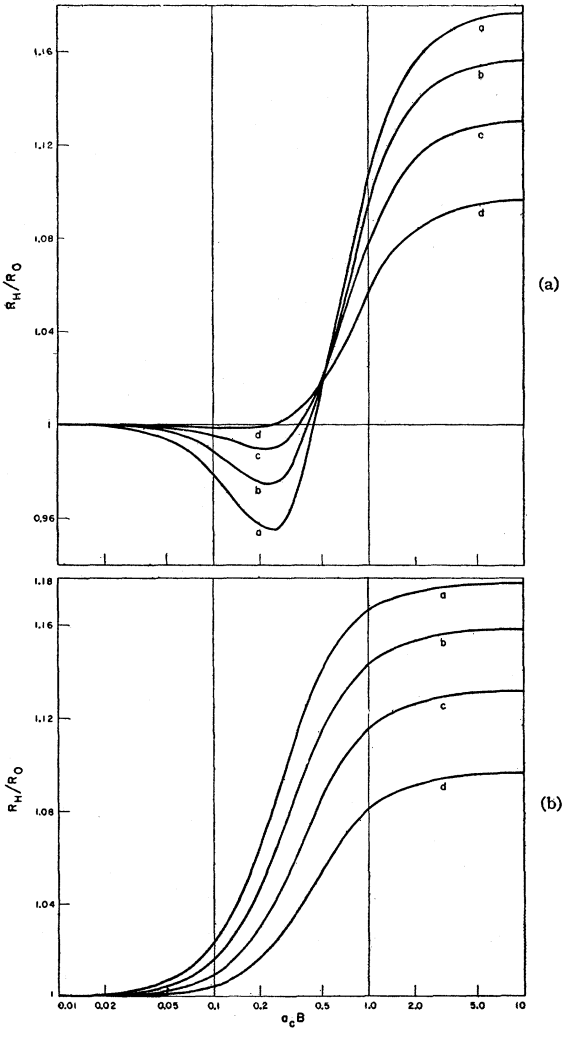

FIG. 3. (a) Field dependence of the normalized Hall coefficient R_H/R_0 for $J_{[110]}B^{[001]}=J_{[100]}B^{[001]}$. Theoretical—$\tau$=constant; curve a—$K=6.2$, b—$K=5.2$, c—$K=4.2$, d—$K=3.2$. (b) Field dependence of the normalized Hall coefficient R_H/R_0 for $J_{[110]}B^{[\bar{1}11]}$. Theoretical—τ=constant; curve a—$K=6.2$, b—$K=5.2$, c—$K=4.2$, d—$K=3.2$.

assumption, as is well known, is not completely justified,[7] since the energy dependence of the scattering process is different in each case, so that each process will be effective only for the electrons in a particular range of energy. For this work collision frequencies of the form

$$\nu = I\mathcal{E}^{-\frac{1}{2}} + L\mathcal{E}^{\frac{1}{2}} + N \tag{2.5}$$

were used. However, the collision frequencies may also be a function of the direction of motion of the electrons, and therefore separate equations for electrons moving parallel and perpendicular to the major axis of the ellipsoidal energy surface are required.

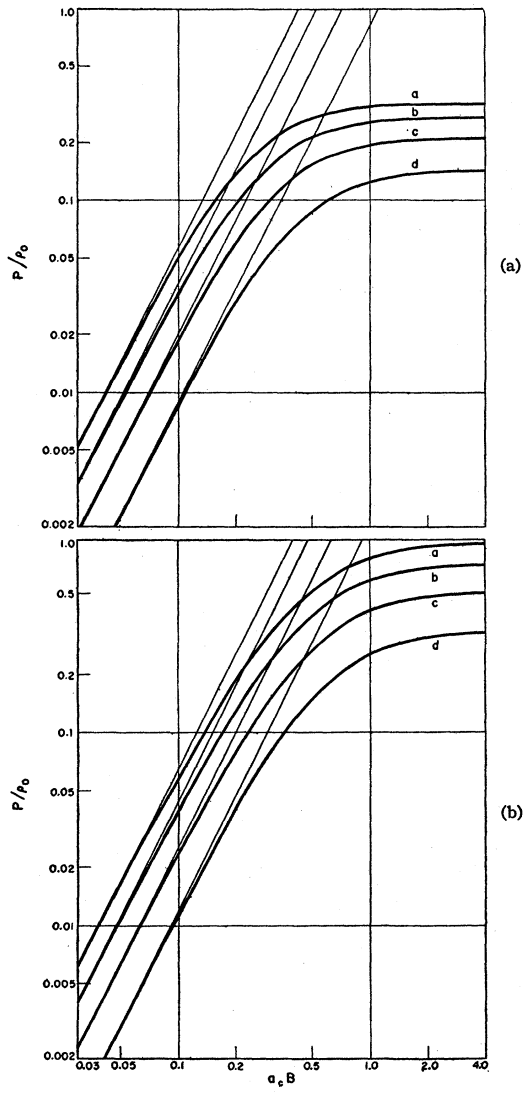

FIG. 4. (a) Field dependence of the planar Hall coefficient P/ρ_0 for $J_{[100]}B^{[110]}$. Theoretical—τ=constant; curve a—K=6.2, b—K=5.2, c—K=4.2, d—K=3.2 (straight lines are the extensions of the low field square law behavior). (b) Field dependence of the planar Hall coefficient P/ρ_0 for $J_{[110]}B^{[010]}$. Theoretical—τ=constant; curve a—K=6.2, b—K=5.2, c—K=4.2, d—K=3.2 (straight lines are the extensions of the low field square law behavior).

Of the three types of scattering under consideration lattice scattering has probably been the most thoroughly investigated. Bardeen and Shockley,[27] using the method of deformation potentials, obtained the expression

$$\tau = \frac{h^4}{8\pi^3}\left(\frac{\rho u_l^2}{kT}\right)\frac{1}{(2m^*)^{\frac{3}{2}}E_1^2}\mathcal{E}^{-\frac{1}{2}} \tag{2.6}$$

for acoustic mode lattice scattering and for spherical energy surfaces, where ρ is the density, u_l the velocity of longitudinal phonons, m^* the density of states effective mass $[(m_l m_t^2)^{\frac{1}{3}}$ for ellipsoids], and E_1 is the shift of the conduction band edge per unit dilation.[28] This equation may be written in the form $1/\tau=\nu=LX^{\frac{1}{2}}$ where X is the reduced energy $\mathcal{E}/kT$, and L is a constant. With $u_l=8.45\times10^5$ cm/sec,[29] $m_l/m_0=0.98$, $m_t/m_0=0.19$[19] where m_0 is the free electron mass, and $E_1=7.0$ ev,[11,27] $L=15.09\times10^{10}$/sec at 77°K and 116×10^{10}/sec at 300°K.

Ionized impurity scattering is calculated by assuming Coulomb interactions, with a cutoff distance equal to the average distance between impurity centers.[12] Brooks and Herring[8] modified the Conwell-Weisskopf formula slightly to take into account screening of the Coulomb scattering potential by the redistribution of the free carriers, and obtained the expression

$$(1/\tau_I) = N_I\pi e^4(m^*)^{-\frac{1}{2}}(2\mathcal{E})^{-\frac{3}{2}}\kappa^{-2}[\ln(1+b)-b/(1+b)],$$

where

$$b = 8\pi(m^*)\kappa kT\mathcal{E}/n'e^2\hbar^2, \tag{2.7}$$

N_I is the number of ionized impurities, m^* the effective mass and κ the dielectric constant. Ham later showed that the anisotropy of the scattering could be considerable for ellipsoidal energy surfaces,[30] and showed that for small angle ionized impurity scattering $\tau_l/\tau_t=4$. Then

$$[\nu_{IL}(\nu_{IT})^2]^{\frac{1}{3}} = \nu_I = 1/\tau_I \quad \text{and} \quad \nu_{IT}/\nu_{IL} = 4, \tag{2.8}$$

where ν_{IL} is the collision frequency for electrons moving along the major ellipsoidal axis and ν_{IT} the collision frequency for electrons moving perpendicular to the major axis. The scattering functions for ionized impurities can then be written[31]

$$\nu_{IL} = I_l X^{-\frac{1}{2}}, \quad \nu_{IT} = I_t X^{-\frac{3}{2}}. \tag{2.9}$$

[27] J. Bardeen and W. Shockley, Phys. Rev. **80**, 72 (1950).

[28] Herring and Vogt[11] later showed that acoustic lattice scattering may be anisotropic. However, to our knowledge there is no data on the anisotropy, which is probably small, and none of the available samples were pure enough to make an estimate. Scattering by optical modes was not considered.

[29] H. J. McSkimin, J. Appl. Phys. **24**, 988 (1953).

[30] F. S. Ham, Phys. Rev. **100**, 1251 (1955).

[31] The energy $\mathcal{E}$ in the expression for b is usually set equal to $3kT$ to simplify the scattering terms. Calculations were made which showed that for samples of moderate resistivity the effect of this was small: a 3% decrease in the resistivity and a 3% increase in low field magnetoresistance, no change in the high field magnetoresistance and less than 1% in the the low field Hall coefficient.

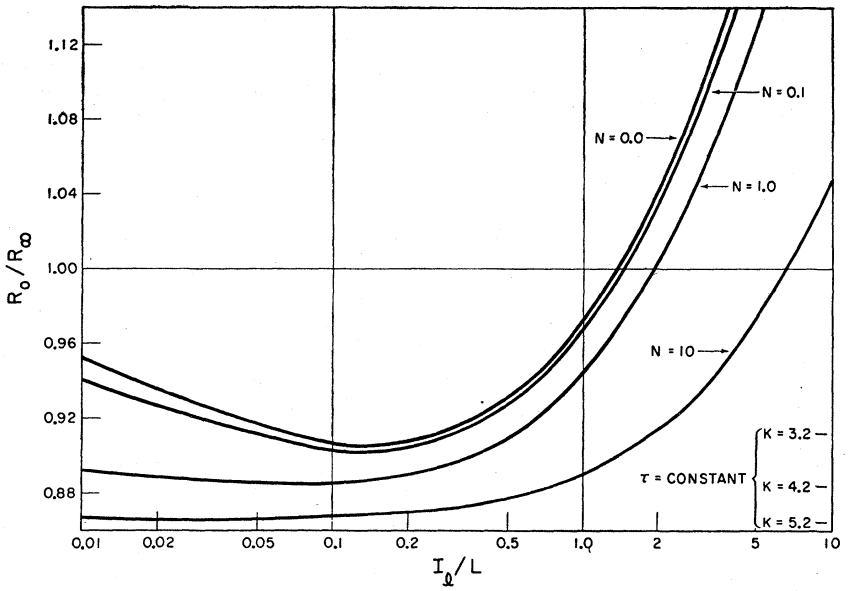

FIG. 5. Ratio of the zero field limit to the infinite field limit of the Hall coefficient R_0/R_∞ as a function of the ratio of ionized impurity to acoustic lattice scattering I_t/L for several values of neutral impurity scattering N. Theoretical—$\tau=\tau(\mathcal{E})$, $K_m=5.2$, $L=1.0$, $I_l/I_t=\frac{1}{4}$.

A simple Hall measurement was used to get the number of ionized impurities, n, N_I was assumed to be equal to the number of free carriers.

The third scattering mechanism to be considered is neutral impurity scattering. Erginsoy showed it to be energy independent on the basis of the scattering of electrons by hydrogen atoms.[14] He obtained the expression

$$\nu_N=1/\tau_{NI}=20\kappa N_n h^3/8\pi^3 m^{*2}e^2=N, \qquad (2.10)$$

where N_n is the number of neutral impurities and N is a constant. Later it was shown that neutral impurity scattering is probably isotropic even for ellipsoidal energy surfaces[9]; and recently Sclar has shown that the scattering is slightly energy dependent.[15] In the calculations Erginsoy's expression was used. N_n was assumed to be zero at 300°K and equal to the difference in the number of free carriers between 300°K and 77°K at liquid nitrogen temperature.

With these expressions for the scattering mechanisms we can write:

$$\begin{aligned}\nu_l&=I_l X^{-\frac{3}{2}}+LX^{\frac{1}{2}}+N,\\ \nu_t&=I_t X^{-\frac{3}{2}}+LX^{\frac{1}{2}}+N,\end{aligned} \qquad (2.11)$$

which are the expressions to be substituted in Eq. (2.3) for the conductivity components.

Figures 5, 6, 7, 8, and 9 show the behavior of the Hall coefficient and magnetoresistance when the scattering functions are of the type just described. For all the figures a mass anisotropy $K=5.2$ was used, and with the exception of Figs. 6(a) and 8(a) the anisotropy of the ionized impurity scattering was 4 ($I_t/I_l=4$). The abscissa scale is given in terms of $a_0B=eB\tau_0/m_l$ where τ_0 is a constant.

Figure 5 shows the dependence of the ratio of the low field limit R_0 to the high field limit R_∞ of the Hall coefficient on the relative amounts of the three types of scattering. The ionized impurity scattering increases toward the right. Note the ratios of R_0/R_∞ for the constant τ calculations in the lower right hand corner.

Figure 6(a) shows the effect of an anisotropy in the ionized impurity scattering on the field dependence of the Hall coefficient. In Fig. 6(a), curve b is for isotropic scattering, curve a was calculated with $I_t/I_l=4$, and curves c and d were calculated with anisotropies which increase the total anisotropy, $K=K_mK_\tau$. Notice the similarity of these curves to those of Fig. 3(a), which show the effect of the mass anisotropy.

The strong dependence of the Hall coefficient on the relative amounts of ionized impurity and lattice scattering is shown in Fig. 6(b) and 6(c). It should be emphasized that the high field limit and not the low field limit is independent of the scattering functions. It is evident from Fig. 6(b) that the depth of the minimum in the normalized Hall coefficient is a function of the relative amount of ionized impurity scattering. This effect has been plotted in Fig. 7. The curve disappears at the right as the zero field value of the Hall coefficient normalized to the high field limit R_0/R_∞ rises rapidly at high concentrations of ionized impurities and the minimum is washed out. Included in Fig. 7 are the depths of the minima for the constant τ calculations.

In Fig. 8 the magnetoresistance versus magnetic field is plotted for the same conditions as used for the calculations of the Hall coefficient shown in Fig. 8. Figure 8(a) shows that a change of the anisotropy of the ionized impurity scattering has much the same effect on the magnetoresistance as a change in the mass anisotropy (Fig. 1). Figure 8(b) shows some results that were quite surprising. The decrease in the low field magnetoresistance coefficient as the total scattering is increased is as expected (Fig. 9), however it is difficult

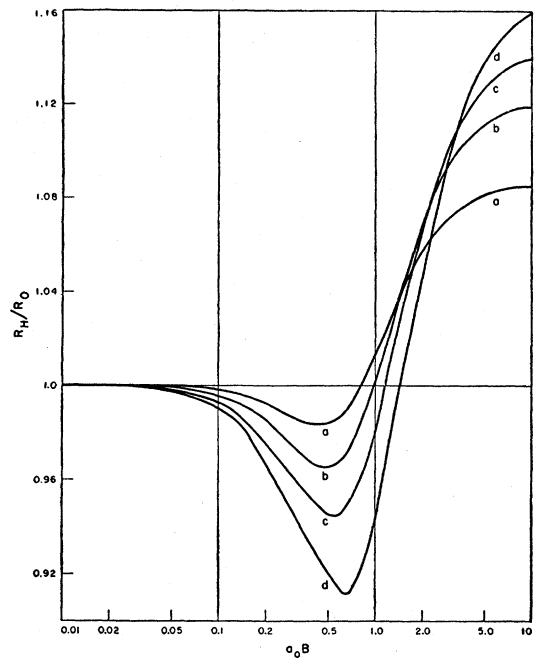

(a)

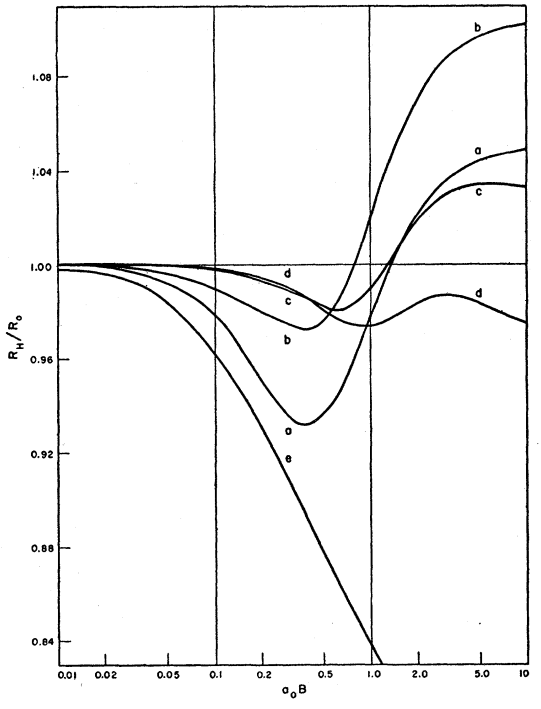

(b)

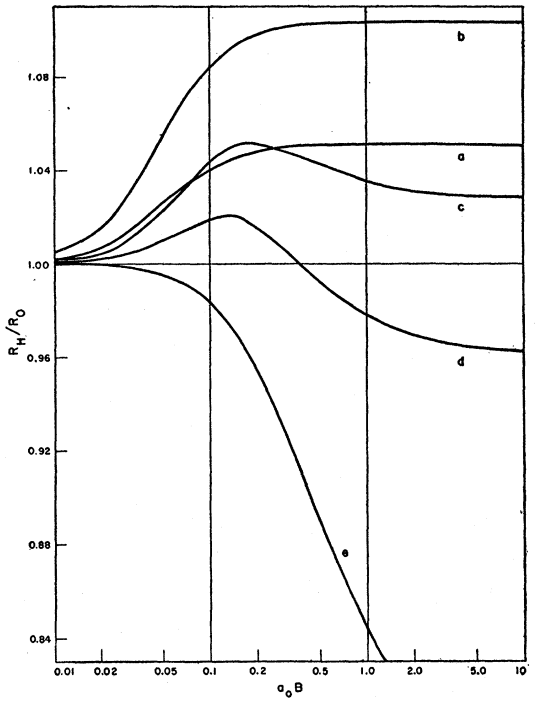

(c)

FIG. 6. (a) Field dependence of the normalized Hall coefficient R_H/R_0 for $J_{[110]}B^{[001]}$. Theoretical—$\tau=\tau(\varepsilon)$, $K_m=5.2$, $L=1.0$, $N=0$, $(I_l)(I_t)^2=1$. I_l/I_t=in curve a—$\frac{1}{4}$ ($R_\infty/R_0=1.0857$), b—1 ($R_\infty/R_0=1.1211$), c—$\frac{1}{2}$ ($R_\infty/R_0=1.1431$), d—$\frac{1}{4}$ ($R_\infty/R_0=1.1665$). (b) Field dependence of the normalized Hall coefficient R_H/R_0 for $J_{[110]}B^{[001]}$. Theoretical—$\tau=\tau(\varepsilon)$, $K_m=5.2$, $L=1.0$, $N=0$, $I_l/I_t=\frac{1}{4}$. I_l=in curve a—0.01, b—0.1, c—1.0, d—2.0, e—10.0. $R_\infty/R_0=a$—1.0511, b—1.1034, c—1.0287, d—0.9628, e—0.7696. (c) Field dependence of the normalized Hall coefficient R_H/R_0 for $J_{[110]}B^{[\bar{1}11]}$. Theoretical—same as Fig. 6(b).

to see why the high field magnetoresistance should first decrease and then increase as the amount of ionized impurity scattering is increased.

The dependence of the low field magnetoresistance coefficient $(\Delta\rho/\rho_0)/(a_0B)^2$ on the total scattering is shown in Fig. 9. The lattice scattering constants were not changed in the calculations for this figure. The highest curve is for the least (none) neutral impurity scattering, and low amounts of ionized impurity scattering are at the left.

Many of the low and intermediate field effects can be shown experimentally but unfortunately most of

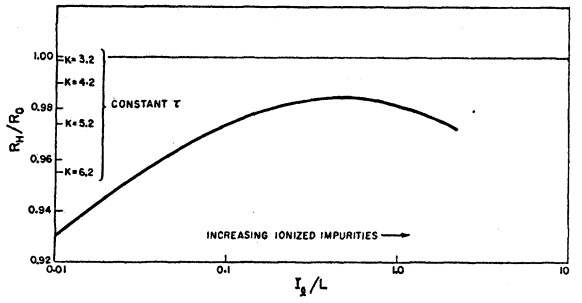

FIG. 7. The minimum value of the normalized Hall coefficient R_H/R_0 as a function of the ratio of ionized impurity to lattice scattering I_I/L. Theoretical—$\tau=\tau(\mathcal{E})$, $K_m=5.2$, $I_t/I_I=4.0$, $N=0$, $J_{[110]}B^{[001]}$. Constant τ values for various K are shown at left.

the high field effects are beyond the reach of the available magnetic fields. As we shall see, while the experimental agreement with the calculations is not perfect, they do show all of the qualitative phenomena, at least up to the highest available fields.

Results can also be calculated as above for the angular dependences of the magnetoresistance and Hall coefficients. However, these changes with scattering are relatively small and nowhere near as prominent as the scattering dependence of. for example, the Hall coefficient.

IV. EXPERIMENTAL

The experimental arrangement was straightforward.[18] The galvanomagnetic potentials were measured with a Rubicon Type B potentiometer. The magnetic fields were supplied by a Varian 12-in. electromagnet with cone shaped polefaces having 3-in. flats and a $1\frac{3}{4}$-in. gap, and measured by means of a U. S. Navy LM18 frequency meter and a nuclear resonance magnetometer. With this arrangement the precision of the measurements is estimated at 0.01%. Constant temperatures were maintained by using a liquid N_2 bath for the 77°K measurements and circulating water from a constant temperature bath for the 300°K measurements. The temperatures were constant to better than ±0.1°C. The samples (Fig. 10), shown mounted on a teflon sample holder, were cut with an ultrasonic die to the desired shape. The central region was a rod one millimeter square in cross section and about 8 mm long, having side contacts the thickness of the sample and a width of 0.003 in.–0.006 in. Ohmic electrical contacts were produced by gold bonding.[32,33] The sample holder was designed so that the samples could be rotated in the magnetic field around each of its principal axes, where the angle was measured with a pointer and protractor after calibration for each sample by a zero of the Hall coefficient or an extremum in the magnetoresistance. For each orientation and field four measurements $(\pm B, \pm I)$ of the galvanomagnetic potentials were made in order, and the results averaged, to minimize the thermal effects and to eliminate errors due to misplacement of the contact areas. The silicon was n-type, arsenic doped, and except for sample 2960, was supplied by the Bell Telephone Laboratories, and the sample parameters are given in Table I.

V. RESULTS

Figure 11 shows the angular dependence of the magnetoresistance for the current in the [100] and [110] directions at 300°K and 77°K. Both sets of measurements were taken at 20 kilogauss. In the figures the experimental points are shown, the solid lines were calculated using a constant τ, with the experimental and calculated values matched when the

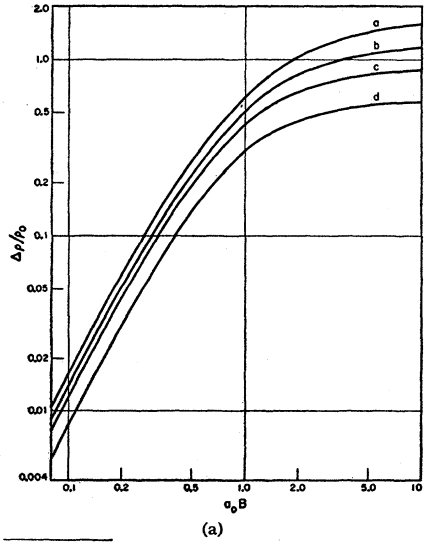

(a)

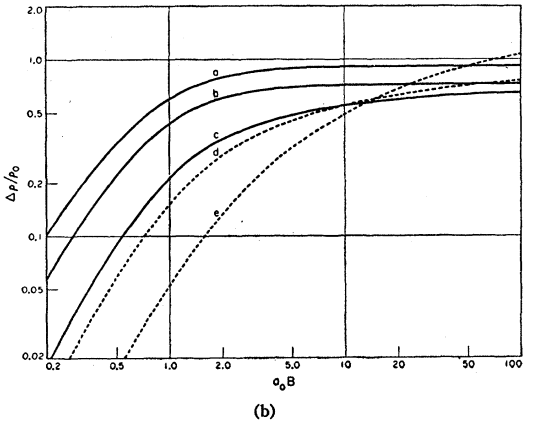

(b)

FIG. 8. (a) Field dependence of the magnetoresistance $\Delta\rho/\rho_0$ for $J_{[110]}B^{[001]}$. Theoretical $-\tau=\tau(\mathcal{E})$, $K_m=5.2$, $L=1.0$, $N=0$, $I_I(I_t)^2=1$. I_t/I_I=in curve a—$\frac{1}{4}$, b—$\frac{1}{2}$, c—1, d—4. (b) Field dependence of the magnetoresistance $\Delta\rho/\rho_0$ for $J_{[110]}B^{[001]}$. Theoretical — $\tau=\tau(\mathcal{E})$, $K_m=5.2$, $L=1.0$, $N=0$, $I_I/I_t=\frac{1}{4}$. I_I=in curve a—0.01, b—0.1, c—1.0, d—2.0, e—10.0.

[32] P. Debye (private communication).
[33] M. Tanenbaum (private communication).

TABLE I. Sample characteristics.

Sample No.	Crystal No. and supplier	Doping	Growth axis	Growth method	Direction of J	Direction of V_H or V_P
2569A-1	Bell XS2860B	As	[100]	Rotated	[100]	[010]
2569B-2	Bell XS2860B	As	[100]	Rotated	[110]	[$\bar{1}$10]
2960	Merck 34S	As	[100]		[110]	[$\bar{1}$10]
2807B-2	Bell 198A	As	[110]	Rotated 60 rpm	[110]	[$\bar{1}$10]
2806B-1	Bell 199A	As	[110]	Rotated 60 rpm	[110]	[$\bar{1}$10]
2807A-2	Bell 198A	As	[110]	Rotated 60 rpm	[110]	[001]

Sample No.	300°K Parameters: Approximate ρ_0(ohm cm)	300°K Parameters: R_0 cm³/coul	300°K Parameters: $\mu_H$cm²/volt sec	77°K Parameters: Approximate ρ_0(ohm cm)	77°K Parameters: R_0 cm³/coul	77°K Parameters: $\mu_H$cm²/volt sec
2569A-1	2.0	-3.5×10^3	1700	0.73	-8.3×10^3	11 400
2569B-2	3.3[a]	-4.7×10^{3}[a]	1430[a]	0.66[b]	-7.9×10^{3}[b]	12 000[b]
2960	27	-4.7×10^4	1770	3.0	-5.2×10^4	17 000
2807B-2	1.9	-3.3×10^3	1750	0.51	-6.8×10^3	13 400
2806B-1	0.22	-3.2×10^2	1440	0.17	-1.5×10^3	8 900
2807A-2				0.57	-7.4×10^3	13 000

[a] Between first and second heating process.
[b] After second heating process.

magnetic field was in an [001] direction. As is seen in the figures the constant mean free time calculation shows all of the symmetries found in the measurements.

Figure 12 shows an attempt at a more quantitative calculation using a constant collision frequency. For these calculations a magnetoresistance vs magnetic field measurement was made and the results compared with Fig. 1 to get a best fit and a relationship between a_cB and the magnetic field. The value of a_c was then used to calculate the curves in Fig. 12. The numbers used in the calculations are given in Table II. Again the constant τ curves show all of the qualitative features of the experimental data. Figure 13 is a comparison of the measurements and the calculations for the normalized Hall coefficient. The same constants as in Fig. 12 were used in the calculations. A curve for $K=3.2$ is also shown which seems to fit the Hall data much better. However, with $K=3.2$ none of the magnetoresistance data would fit at all.

In Figs. 14, 15, 16, 17, 18 the experimental results on a set of three samples of different resistivities measured at 77°K and 300°K are shown. In these figures as elsewhere the points are experimental and the solid lines are the results of calculations. The numbers used in the calculations were derived on the basis of an energy dependent relaxation time and are given in Table II. To plot the figures, curve b in Fig. 14(a) and the measurements of the normalized Hall coefficient for sample 2807B-2 were matched to get the constant a_0. This value of a_0 was then used to plot all of the field de-

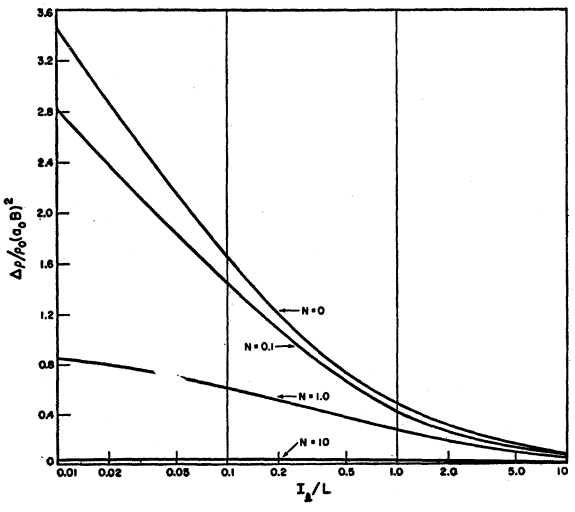

FIG. 9. Limit of the magnetoresistance coefficient $(\Delta\rho/\rho_0)/(a_0B)^2$ as $(h\tau_0)\to 0$ as a function of the ratio I_t/L for several values of N for $J_{[110]}B^{[001]}=J_{[100]}B^{[001]}$. Theoretical—$\tau=\tau(\mathcal{E})$, $K_m=5.2$, $L=1.0$, $I_t/I_l=4$.

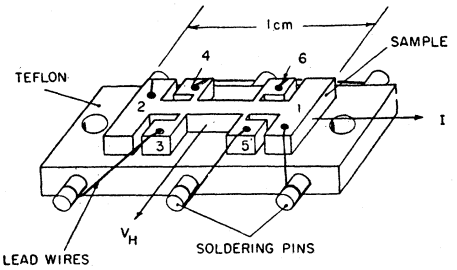

FIG. 10. Sample and sample mounting.

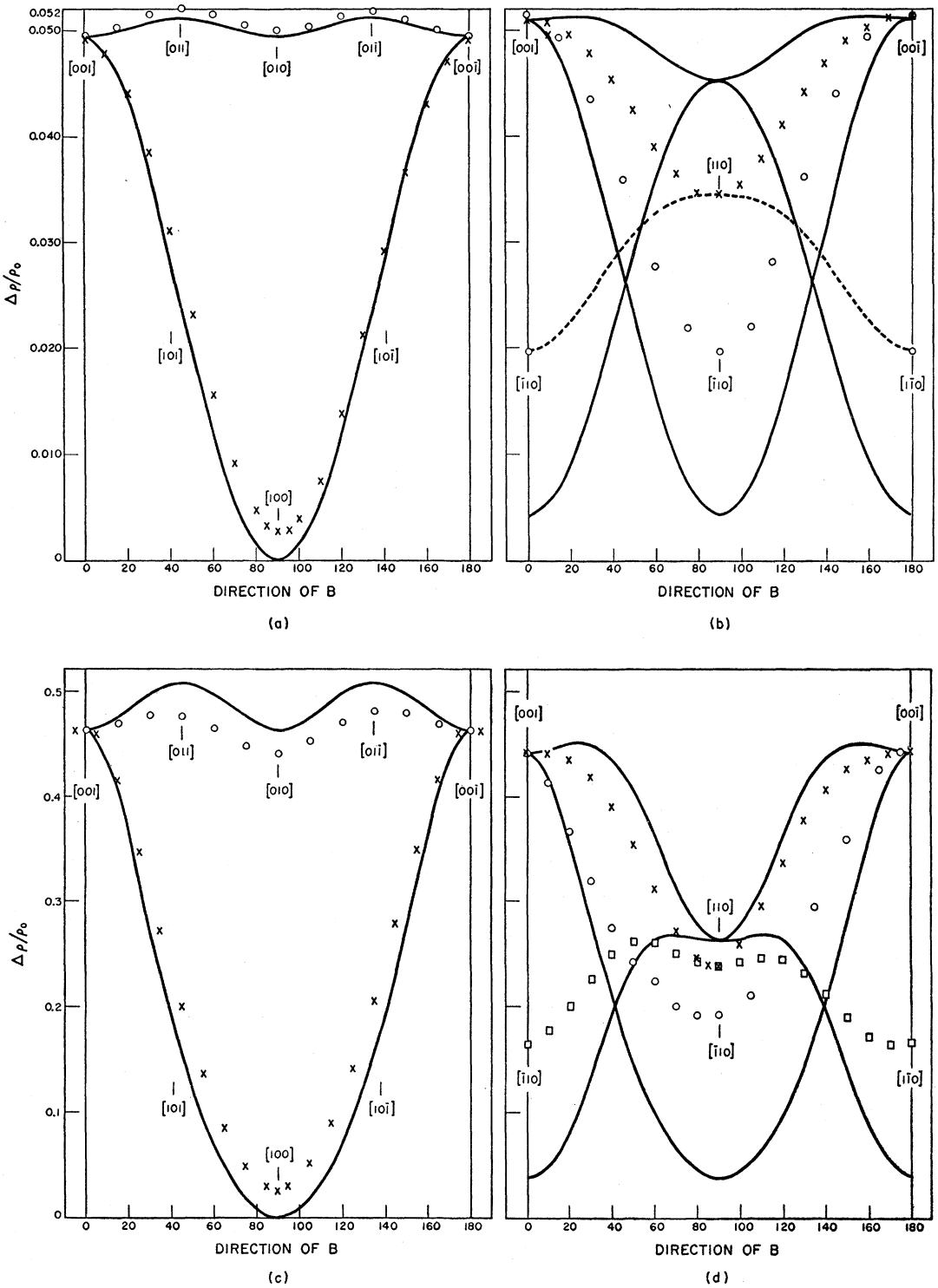

FIG. 11. (a) Angular dependence of the magnetoresistance $\Delta\rho/\rho_0$ at 20 kilogauss. The cardinal directions of the magnetic field B are indicated. Sample 2569A-1, $T=300°K$. The experimental points are for J in a [100] direction; ○ are the points for B in a (100) plane; × are the points for B in a (010) plane. The solid line was calculated with the parameters given in Table II. (b) Angular dependence of the magnetoresistance $\Delta\rho/\rho_0$ at 20 kilogauss. The cardinal directions of the magnetic field B are indicated. Sample 2569B-2, $T=300°K$. The experimental points are for J in a [110] direction; ○ are the points for B in a (110) plane; × are the points for B in a $(1\bar{1}0)$ plane; the magnetoresistance for B in a (001) plane is indicated by the dashed line. The solid lines were calculated with the parameters given in Table II. (c) Angular dependence of the magnetoresistance $\Delta\rho/\rho_0$ at 20 kilogauss. The cardinal directions of the magnetic field

TABLE II. Compilation of numbers used for comparisons of experimental data and theoretical calculations.

Figures	
11	τ=constant, K=5.2, B=20 kilogauss
	11a a_cB=0.112
	11b a_cB=0.114
	11c a_cB=0.597
	11d a_cB=0.560
12	τ=constant, K=5.2, a_c=0.0305/kilogauss
	curve a—B=20 kilogauss, a_cB=0.610
	curve b—B= 4 kilogauss, a_cB=0.122
	curve c—B=10 kilogauss, a_cB=0.305
13	τ=constant, K=3.2 and 5.2, a_c=0.0305/kilogauss
14–17	$\nu=\nu(\varepsilon)$, K_m=5.2, a_0=0.9/kilogauss when $\tau_0=10^{-10}$ sec.
	For 77°K data (Figs. 14, 16) the numbers used in Eq. (2.11) for $\nu=\nu(X)$ are:

Curve	Sample No.	I_1	L	N	I_t
a	2960	0.944	15.09	0.0064	3.776
b	2807B-2	5.58	15.09	1.6409	22.32
c	2806B-1	19.58	15.09	6.974	78.33

For 300°K data (Figs. 15, 17) the numbers used in Eq. (2.11) for $\nu=\nu(X)$ are:

Curve	Sample No.	I_1	L	N	I_t
a	2960	0.164	116.0	0	0.655
b	2807B-2	1.903	116.0	0	7.612
c	2806B-1	14.691	116.0	0	58.764

18a,b	$\nu=\nu(\varepsilon)$, K_m=5.2. Use numbers listed above under 77°K in Eq. (2.11) for $\nu=\nu(X)$
	curve b—sample 2807B-2 a_0B=40
	curve c—sample 2806B-1 a_0B=22
18c,d	$\nu=\nu(\varepsilon)$, K_m=5.2. Use numbers listed above under 300°K in Eq. (2.11) for $\nu=\nu(X)$
19a	curve a—sample 2960 a_0B=15.3
	curve b—sample 2807B-2 a_0B=16.4
	curve c—sample 2806B-1 a_0B=15.2

pendent data, both for the Hall coefficient and the magnetoresistance and at both temperatures. For the angular data on the magnetoresistance the value of a_0B was chosen to make the measurements and the computed results coincide in the [001] direction of the magnetic field. As can be seen from Fig. 16(a) no value of a_0B was able to give the measured value of magnetoresistance at 20 kG for sample 2960. Therefore no angular calculations were made for sample 2960 for Fig. 18.

Figure 19(a) shows the planar Hall coefficient as a function of angle at 300°K. The numbers used for numerical calculations were the same as those used for Fig. 18(d). The planar Hall measurements at 77°K on these samples showed considerable distortion shown in Fig. 19(b), apparently due to inhomogeneities, and were not calculated.

VI. DISCUSSION

Experimental measurements of the galvanomagnetic coefficients have been compared with the results of calculations using both an energy independent and an energy dependent anisotropic collision frequency. The constant collision frequency calculations showed all the qualitative features of the experimental results, including both the symmetries and the field dependent effects. Since the symmetry and field effects depend strongly on the structure of the band edges it is apparent that because of their simplicity, the constant τ approximation should be useful in exploratory work on band structure in many materials.

However, because there is no way, with a constant collision frequency, to explain either the temperature or resistivity dependence of the galvanomagnetic coefficients, if quantitative accuracy is desired it is necessary to turn to an approximation which is closer to the physical situation. As has been shown above an energy dependent anisotropic collision frequency which depends on such factors as the temperature, type and amount of impurities, the scattering anisotropy and the mass anisotropy can be used to predict more accurately the experimental results. However, the calculations are lengthy and must be performed with the aid of a large computer. Considering the number of

B are indicated. Sample 2569A-1, T=77°K. The experimental points are for J in a [100] direction; ○ are the points for B in a (100) plane; × are the points for B in a (010) plane. The solid lines were calculated with the parameters given in Table II. (d) Angular dependence of the magnetoresistance $\Delta\rho/\rho_0$ at 20 kilogauss. The cardinal directions of the magnetic field B are indicated. Sample 2569B-2, T=77°K. The experimental points are for J in a [110] direction; ○ are the points for B in a (110) plane; × are the points for B in a $(\bar{1}10)$ plane; and □ are the points for B in a (001) plane. The solid lines were calculated with the parameters given in Table II.

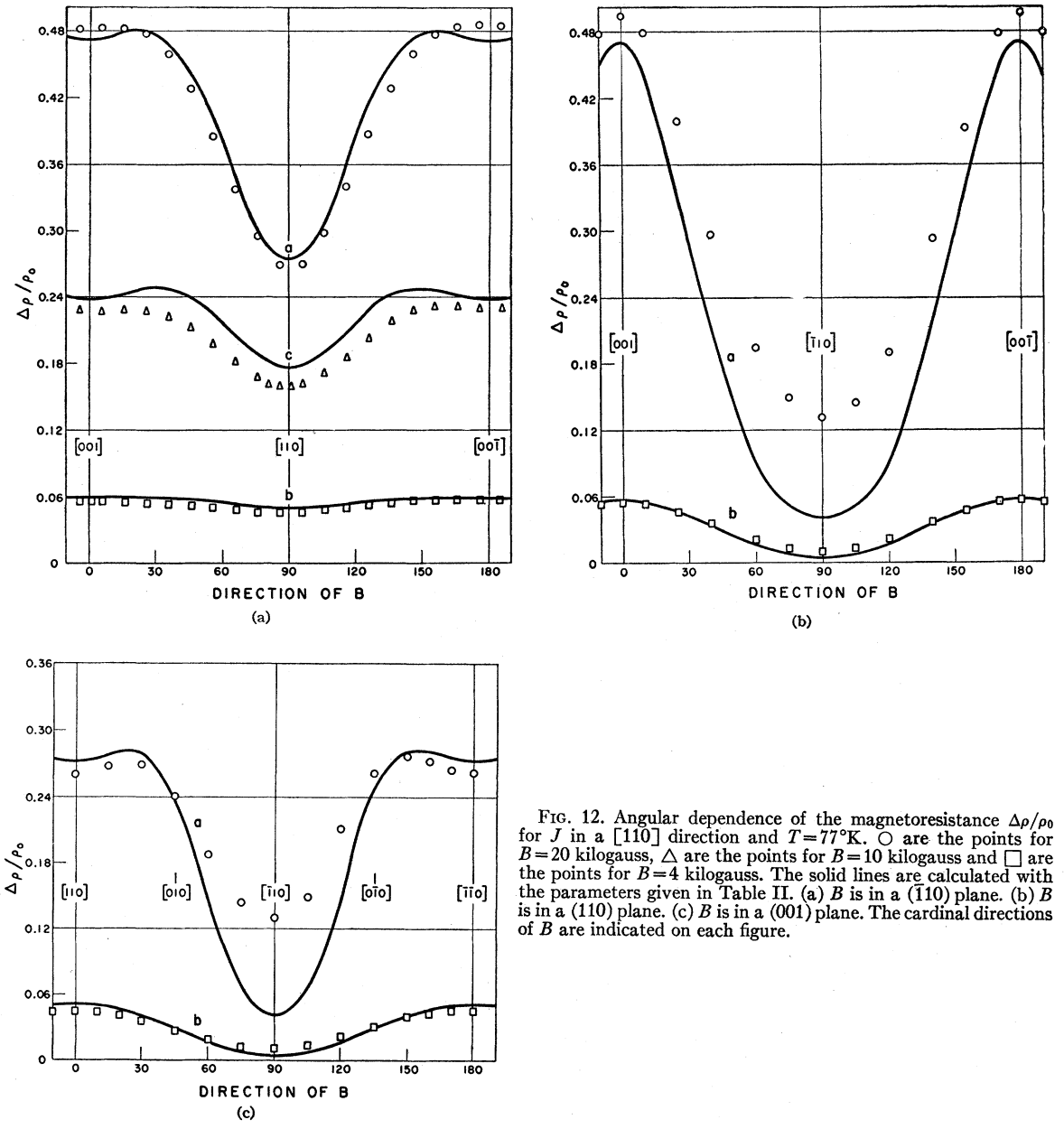

FIG. 12. Angular dependence of the magnetoresistance $\Delta\rho/\rho_0$ for J in a [110] direction and $T=77°K$. ○ are the points for $B=20$ kilogauss, △ are the points for $B=10$ kilogauss and □ are the points for $B=4$ kilogauss. The solid lines are calculated with the parameters given in Table II. (a) B is in a (110) plane. (b) B is in a (110) plane. (c) B is in a (001) plane. The cardinal directions of B are indicated on each figure.

parameters which go into the calculation, and affect the results, it is difficult to justify this type of calculation except in substances which have already been fairly thoroughly investigated. If one were able to obtain samples in which a single type of scattering was predominant, it would be possible to isolate and measure the various parameters one at a time. However, very pure material is usually unavailable, and large numbers of impurities often affect the band structure itself.

As was shown in Sec. II, the galvanomagnetic coefficients can be calculated without the use of any adjustable parameters. However, for most samples (except Sample 2960 at 77°K and high fields) the calculated magnetoresistance for J [110] and B [001], (transverse orientation) was always higher than the measured values which implies that there is considerably more scattering than has been calculated. Actually there are a number of scattering sources which have not been considered, such as the probable existence of minority impurities contributing to the ionized impurity scattering, and the presence of neutral impurities such as oxygen or nitrogen.[34] For this reason, only the relative values of the amounts of scattering of different types was used. It is worth noting, however,

[34] W. Kaiser, Phys. Rev. **105**, 1751 (1957).

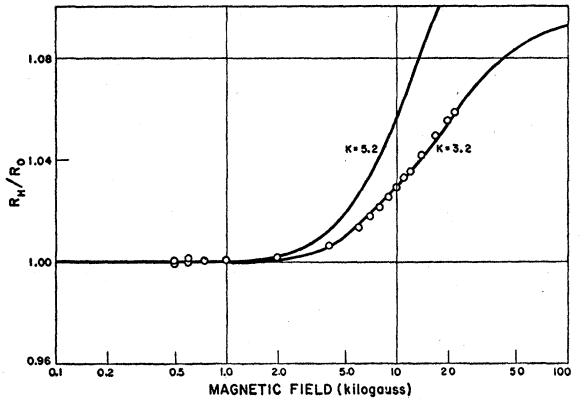

FIG. 13. Field dependence of the normalized Hall coefficient R_H/R_0 for $J_{[110]}B^{[\bar{1}10]}$. Experimental—$T=77°$K. Sample 2807A-2. Theoretical—see Table II.

that for all of the field dependent results at both temperatures, a single value of the parameter a_0 was sufficient.

The anisotropy of the magnetoresistance, which is less than calculated, could probably be explained by an anisotropy in the lattice scattering. This anisotropy

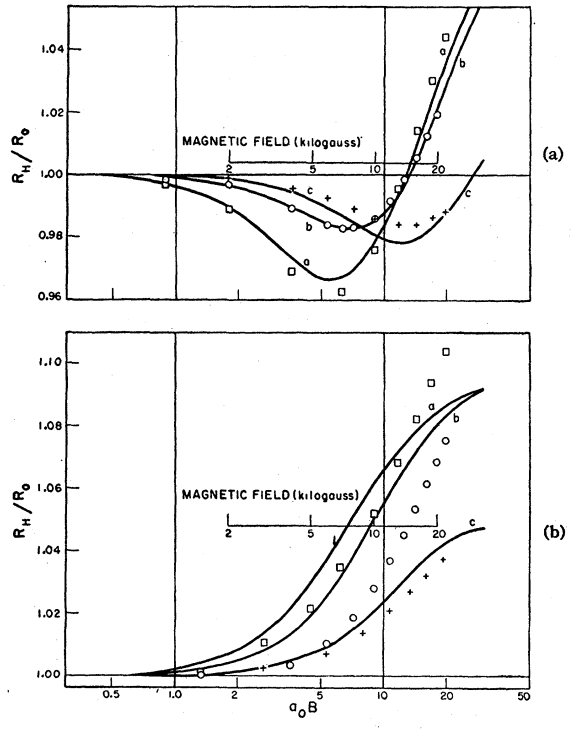

FIG. 14. Field dependence of the normalized Hall coefficient R_H/R_0 for J in a [110] direction and $T=77°$K. □—Sample 2960, ○—Sample 2807B-2, +—Sample 2806B-1. The solid lines were calculated with the parameters given in Table II. (Measurements of the Hall coefficients were made from 0.4 to 22 kilogauss. The low field values form a straight line as indicated by the theoretical curves. They have been left off the curves presented here for reasons of clarity). (a) B is in a [001] direction. (b) B is in a [$\bar{1}$11] direction.

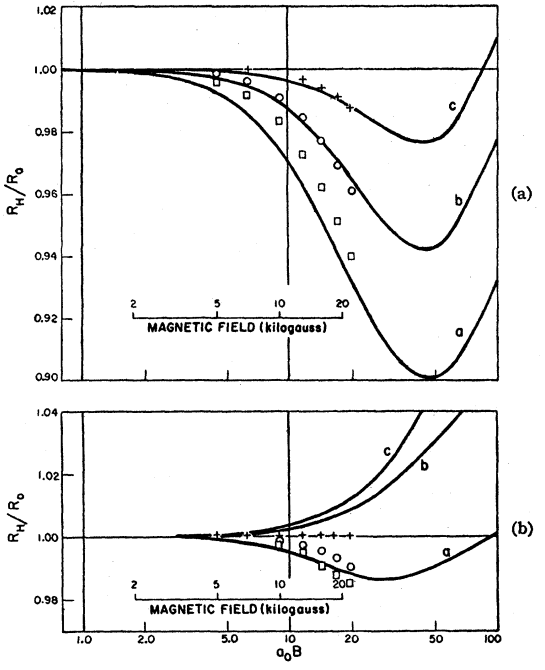

FIG. 15. Field dependence of the normalized Hall coefficient R_H/R_0 for J in a [110] direction and $T=300°$K. □—Sample 2960, ○—Sample 2807B-2, +—Sample 2806B-1. The solid lines were calculated with the parameters given in Table II. (a) B is in an [001] direction. (b) B is in an [$\bar{1}$11] direction.

is probably in such a direction as to reduce the anisotropy ratio $K=K_mK_\tau$, or $K_\tau=\tau_t/\tau_l<1$. In relatively pure samples a small anisotropy in the lattice scattering has a much greater effect than an anisotropy in the ionized impurity scattering. None of the samples available were so pure as to allow neglect of ionized impurity scattering and allow an experimental determination of the anisotropy in the lattice scattering. A single calculation of the angular dependence of the magnetoresistance was performed with $K_\tau=\tau_t/\tau_l=1/1.1$ for acoustic lattice scattering. This change had a considerable effect on the angular curves, and little effect on the field dependent curves. Only a small anisotropy in the lattice scattering would be needed to fit the experimental data.

Experimentally, the difficulty seems to lie in the samples and not in the measurements. Care was taken to be sure the samples were oriented properly, temperatures were carefully regulated, and the potentials were accurately measured. Any surface effects with the fairly low resistivities of these samples should be small—we detected no such effects. It is probable that inhomogeneities in the samples affected the measurements. There seems to be no other way to explain the planar Hall measurements shown in Fig. 19(b), or the asymmetry of the magnetoresistance in Fig. 18(b), which is probably a contribution from the planar Hall effect. In regard to this, many samples during the beginning

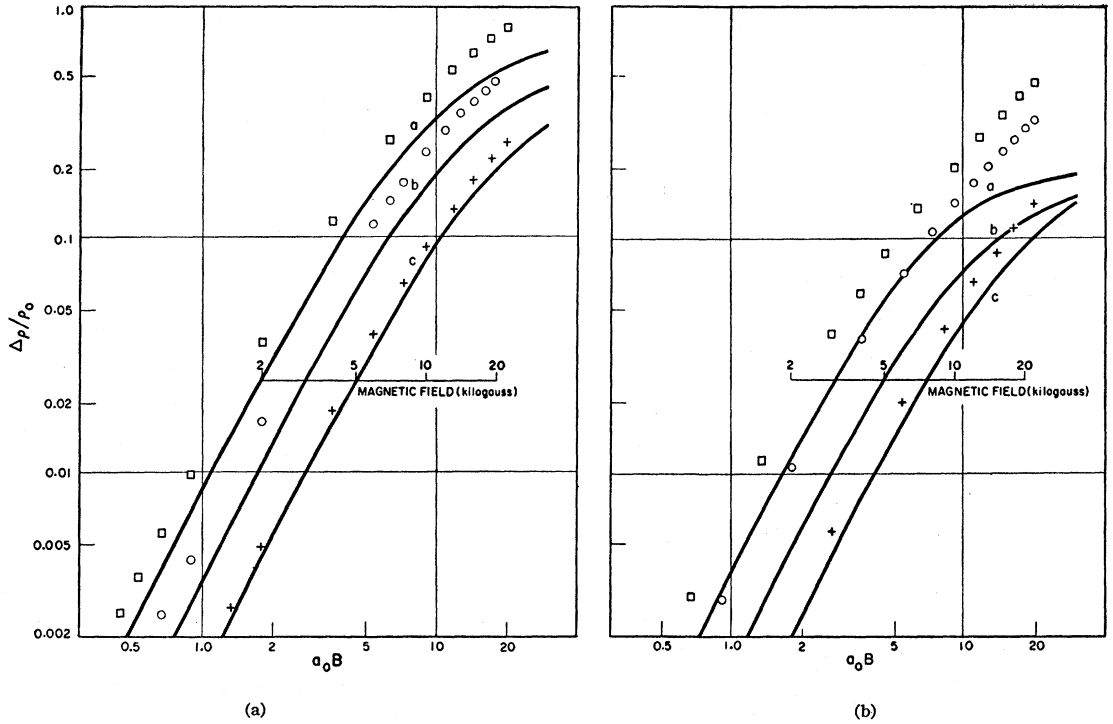

FIG. 16. Field dependence of the magnetoresistance $\Delta\rho/\rho_0$ for J in a [110] direction and $T=77°K$. □—Sample 2960, ○—Sample 2807B-2, +—Sample 2806B-1. The solid lines were calculated with the parameters given in Table II. (a) B is in an [001] direction. (b) B is in an $[\bar{1}11]$ direction.

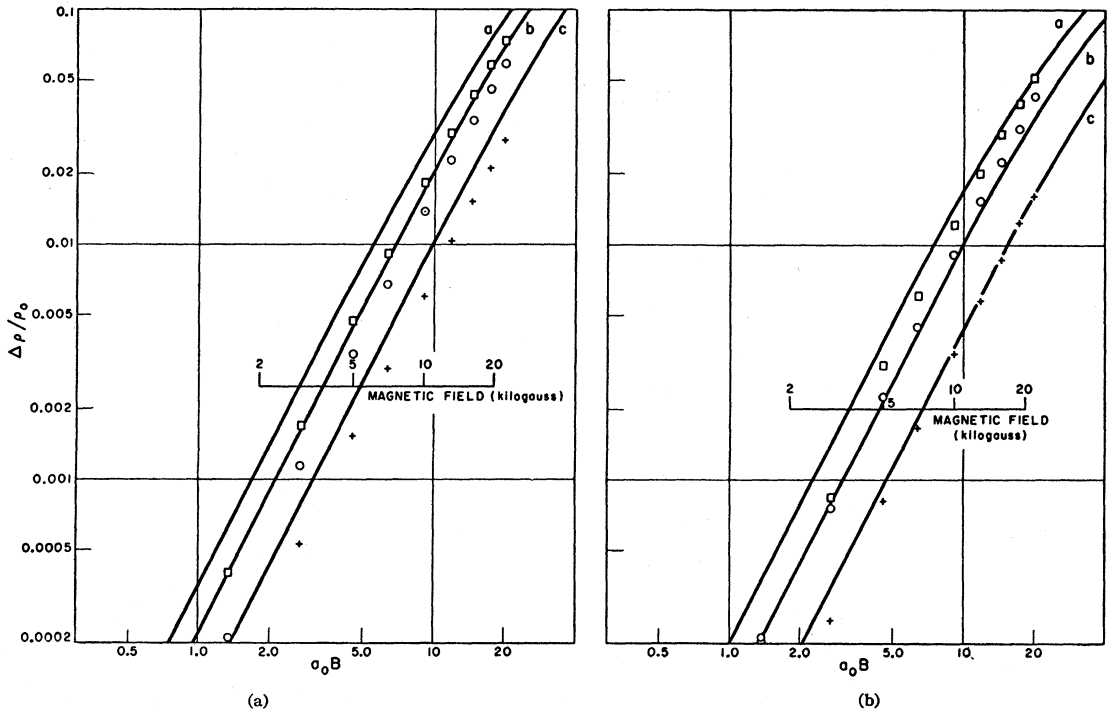

FIG. 17. Field dependence of the magnetoresistance $\Delta\rho/\rho_0$ for J in a [110] direction and $T=300°K$. □—Sample 2960, ○—Sample 2807B-2, +—Sample 2806B-1. The solid lines were calculated with the parameters given in Table II. (a) B is in an [001] direction. (b) B is in an $[\bar{1}11]$ direction.

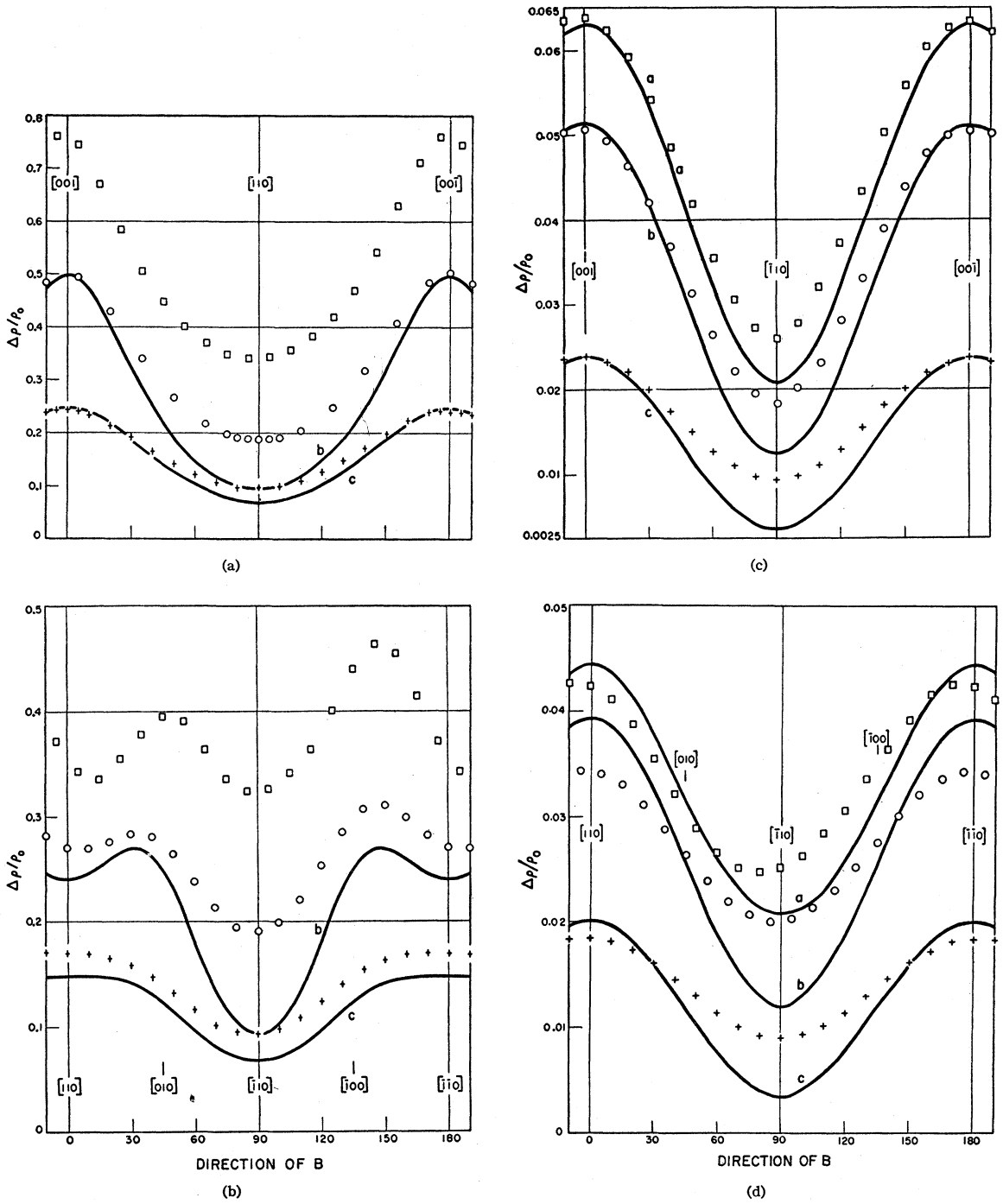

FIG. 18. Angular dependence of the magnetoresistance for J in a [110] direction and an applied magnetic field of 20 kilogauss. □—Sample 2960, ○—Sample 2807B-2, +—Sample 2806B-1. The solid lines were calculated with the parameters given in Table II. (a)—$T=77°K$, B is in a (110) plane. (b)—$T=77°K$, B is in a (001) plane. (c)—$T=300°K$, B is in a (110) plane. (d)—$T=300°K$, B is in a (001) plane.

stages of this experiment were heated to 750–850°C in a hydrogen atmosphere and then cooled very slowly (12 hours). In none of these samples were there large distortions of the measured curves such as are seen in Fig. 19(b). The implication is that the heat treatment reduced the inhomogeneities in the material. Herring has also pointed out that the magnetoresistance can be affected by inhomogeneities, particularly in the high

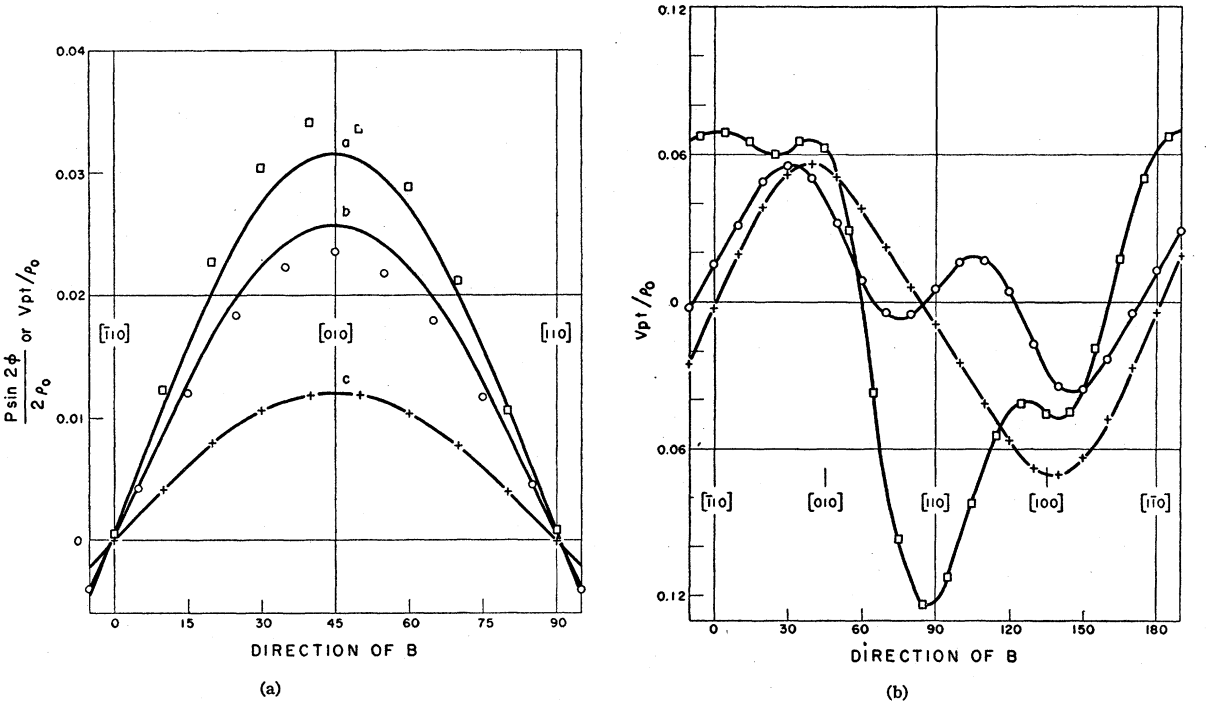

FIG. 19. Angular dependence of the planar Hall coefficient V_{Pt}/ρ_0 at 20 kilogauss for J in a [110] direction and B in an (001) plane. The cardinal directions of the magnetic field B are given. □—Sample 2960, ○—Sample 2807B-2, +—Sample 2806B-1. (a) $T=300°K$. The solid lines were calculated with the parameters given in Table II. (b) $T=77°K$. There are no theoretical curves (see text).

field region.[35] This effect may be enough in some cases to prevent saturation in the high field magnetoresistance. It is possible that this effect may be responsible for the very high (for silicon) magnetoresistance for sample 2960 shown in Fig. 16(a). For the lower values of magnetic field, as was pointed out previously, for most samples the measured magnetoresistance is somewhat smaller than the calculated values.

The fact that the anisotropy in the magnetoresistance is less than was calculated is probably real and not an experimental defect or due to inhomogeneities, since the measurements were consistent for all the samples.

CONCLUSIONS

Using the Boltzmann transport equation coupled with an anisotropic effective mass and an anisotropic energy dependent collision frequency, it appears to be possible to explain, qualitatively, all the measurements of the galvanomagnetic coefficients, both field and angular dependent, and also as a function of resistivity. However, to obtain exact quantitative agreement it will be necessary to begin with very pure material in order to fix some of the parameters, particularly those involved in the acoustic lattice scattering. It is also necessary either to measure and calculate the effects of inhomogeneities or to obtain very uniform material.

It has also been shown that a calculation using a constant collision frequency and an anisotropy ratio, K, is very useful in predicting qualitatively, and to some extent quantitatively, the field and angular dependence of the measured galvanomagnetic potentials to be expected with a particular band edge structure.

ACKNOWLEDGMENTS

The author wishes to acknowledge the contribution of Miss M. Clare Glennon in programming and plotting the many calculations. He also wishes to thank Dr. John Mavroides of Lincoln Laboratory and Professor William P. Allis and Professor Sanborn Brown of the Massachusetts Institute of Technology for many hours of helpful and stimulating discussions. The author is grateful for the samples supplied by Dr. M. Tanenbaum of the Bell Telephone Laboratory. The technical and financial aid received from Lincoln Laboratory while a Staff Associate is gratefully acknowledged by the author.

[35] C. Herring (private communication).